International Conference on Space Optics—ICSO 2022

Dubrovnik, Croatia

3–7 October 2022

Edited by Kyriaki Minoglou, Nikos Karafolas, and Bruno Cugny,

High stability LO generation by injection-locking of hybrid integrated dual InP-Si3N4 laser source for satellite payloads in Ka-, Q-, V-band

International Conference on Space Optics — ICSO 2022, edited by Kyriaki Minoglou, Nikos Karafolas, Bruno Cugny, Proc. of SPIE Vol. 12777, 127774Y · © 2023 ESA and CNES · 0277-786X · doi: 10.1117/12.2690896

High Stability LO Generation by Injection-Locking of Hybrid Integrated Dual InP-Si3N4 Laser Source for Satellite Payloads in Ka-, Q-, V-band

Alberto Zarzuelo*[a], Jessica Cesar [a], Robinson Guzmán [a], Luis Gonzalez [a], Charoula Mitsolidou[b], Roelof Bernardus Timens[b], Víctor Sánchez-Martínez[c], Peter D. H. Maat[b], Paulus W. L. van Dijk[b], Chris G. H. Roeloffzen[b], Guillermo Carpintero[a]
[a]Universidad Carlos III de Madrid, Av. de la Universidad, 30, 28911 Leganés, Spain; [b]LioniX International BV, Hengelosestraat 500, 7521 AN, Enschede, The Netherlands; [b]SENER Aeroespacial S.A., Severo Ochoa 4, 28760 Tres Cantos, Spain
*azarzuel@pa.uc3m.es

ABSTRACT

We propose optical injection locking (OIL) injecting for the first-time a hybrid InP-Si3N4 laser source using another laser integrated on the same chip for microwave generation through optical heterodyning in Ka-, Q- and V-bands. A study of the drift exhibited by the devices will be performed as key parameter of lasers. The amount of free-running drift exhibited by the lasers and a way to minimize as much as possible. According to the measured drift that goes in the worst case up to 520 MHz. However, the electric drift of the beat-note RF signal keeps below 50 MHz thanks of being thermally stabilize over the same conditions. To eliminated the drift, an optical injection locking of one InP/Si3N4 hybrid integrated laser have been done by injecting another hybrid laser integrated on the same chip for the first time. We have demonstrated a locking range demonstrated a locking range of 1.86 GHz.

Keywords: microwave photonics, integrated microwave photonics, reconfigurable payload, optical injection-locking, optical heterodyning

1. INTRODUCTION

Satellite telecommunications will require an increase of the capacity and the flexibility to attempt the more demanding data bandwidth in the near future. This increase is associate with the need go to higher frequency bands to be able to handle these high data rates. An increase of this capacity is translated into an increase of equipment count, mass & power consumption. The main challenge is to keep the flexibility within a "launchable" volume, mass & power consumption. Microwave Photonics (MWP) has positioned as a promising technology to overcome this challenge. MWP is capable to handle wide bandwidths and system reconfigurability while maintaining low size & compactness. A promising field of application are satellite communications (SATCOMs) [1], powering the novel Very High Throughput Satellites (VHTS), where new technologies are required to increase the capacity and flexibility of the communication payloads [2].

Several research works have reported high level schemes of how a photonic payload looks like [5]. In the Figure 1, we can observe an example of a satellite photonic payload. Basically, they consist in four main blocks. By order in the chain, they are the Photonic Frequency Generation Unit (PFGU), which is basically the generation and distribution of LO throughout the system. The Photonic Frequency Conversion Unit (PFCU) which combines the optical LO with the RF incoming N beams. The Optical Switching Matrix (OSM) that carries-out the optical signal processing of by performing a channel multiplexing or demultiplexing. Finally, the Opto-Electronic Conversion Unit (OECU) that converts the signal from the optical domain back to the electrical domain. Any capacity increase requires moving carrier frequencies to higher bands from the current X-band (8-GHz) to Ka band (24-40 GHz), Q band (33-50 GHZ) or V band (40-75 GHz) [3]. This is directly related with the PFGU module. While these bands are challenging for traditional satellite approaches, MWP enables handling high data rates and high frequencies, as well as enabling reduced size, mass, immunity to EMI and ease of harness routing (by substituting RF coaxial cables by fiber-optic cables) [4].

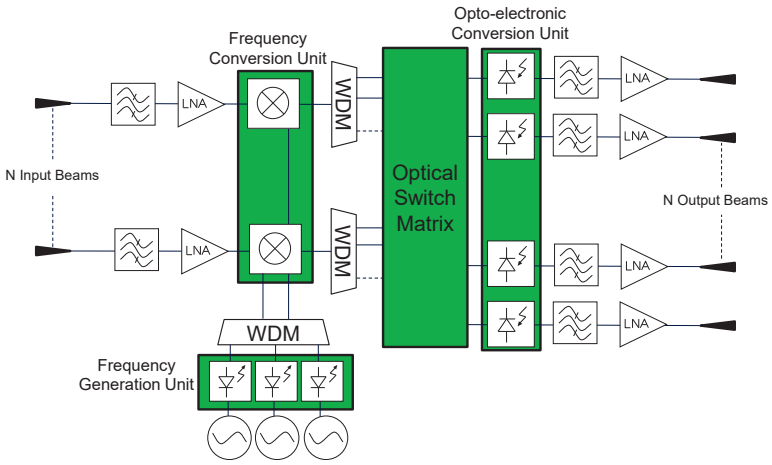

Figure 1. High level block diagram of a satellite photonic payload

A wide range of applications use Microwave Photonics (MWP) technologies to generate radiofrequency (RF) signals. However, over the last years MWP systems and links have relied almost exclusively on discrete components [5], which negatively impacts on their volume and mass producing bulky, expensive and high-power consuming [6]. Photonic integration technology has been recently introduced, coining the term of integrated microwave photonics (iMWP), which offers a significative improvement in terms of size, weight and power (SWaP). In addition, RF signals generated using photonic sources integrated on a Photonic Integrated Circuit (PIC) can provide additional advantages which greatly depend on the RF signal generation technique [7], often based either on short pulse laser sources or on optical heterodyning [[8]].

Several techniques have been reported. The one that provides the greatest flexibility in terms of frequency tunability and the widest RF frequency tuning range [9] is the optical heterodyne. The combination of two semiconductor tunable lasers in an O/E converter with sufficient BW producing a beat note with frequency defined by the wavelength spacing. What is required is a dual wavelength source, producing two optical wavelengths with tunable spacing. The most common approach to dual wavelength sources is to use two single-frequency lasers, at least one of which is wavelength-tunable. The beat note LO that can range from few MHz up to THz range facing the conventional RF LO generators. However, despite of integrating the two lasers on the same chip, the fact that these are two free-running lasers usually results in a large phase noise of the beat note and long-term drift of the frequency [10]. While the two lasers can have very low intrinsic linewidth (less than 1 kHz), the RF beat-note still exhibits a long-term drift due to electrical, thermal & noise instabilities. This issue is not acceptable specially if this drift reaches the range of the RF signal channelizing producing an overlap between different channels. To overcome this problem, different solutions have been proposed, the most usual is using stabilization techniques such as optical injection-locking (OIL) of an optical frequency comb generator. Nevertheless, this solution increases the complexity and degrades the performance in terms of overall SWaP by due to adding additional elements to the system [11].

An alternative approach for the implementation of a dual wavelength source is the optical modulation technique, in which a continuous-wave (CW) single wavelength laser is followed by an optical modulator, usually a Mach-Zehnder modulator (MZM), driven by a Local Oscillator (LO) signal from an electronic RF synthesizer. This technique offers exceptional stability, which is traceable to the LO [[12],[13]]. When the MZM is biased to its minimum transmission point (MTP), the output is a dual sideband with suppressed optical carrier (DSB-SC) which allows generating an RF signal at twice the frequency of the LO, [[9],[14],[15]] and is schematically represented in Fig. 1. The merit of the proposed scheme is that the phase noise of the beat signal is inherited from the RF CW source, being among the schemes that produce the most stable RF signal. The main disadvantage of requiring an RF oscillator at half the target frequency has been addressed through more elaborate structures which provide higher multiplication factors (frequency-doubling [[16]] and quadrupling [[17]])

2. MWP SYSTEM ARCHITECTURE

The MWP filter architecture is shown in Fig. 1. This paper focuses on the frequency generator unit, usually carried-out by a laser, which is the first chain element of the demultiplexer (DEMUX) architecture. A brief description of the MWP system is given next. The laser generates an optical carrier. This carrier is split in two paths. One path directs the light through the Frequency Conversion Unit, usually carried-out by an optical Mach-Zehnder Modulator (MZM), where an incoming RF input Beam in the Ka-, Q-, or V-band is modulated in a double sideband configuration. Then, the optical signal is taken into an optical Single Side Band –Suppressed Carrier filter (SSBSC). The SSBSC filters out the undesired Lower Side Band (LSB) and the optical carrier, while leaves the modulating signal in the optical domain in the Upper Side Band (USB). In this stage, the optical-converted USB signal can be considered as a WDM signal that contains the information of 4 different channels. The USB signal is then processed by the DEMUX channel selector filter, which is responsible of split the information in four separated channels. Afterwards, each demultiplexed channel is combined with the Re-injected "clean" optical carrier, emerging from the second output of the 1:2 splitter. Multiplexing of the USB and Carrier signals is performed by the respective Carrier Re-Injection (CRI) filter. Finally, the resulted optical signals will convert into the RF-domain by an external Photodiode (PD) through the beating, providing RF end-to-end performance.

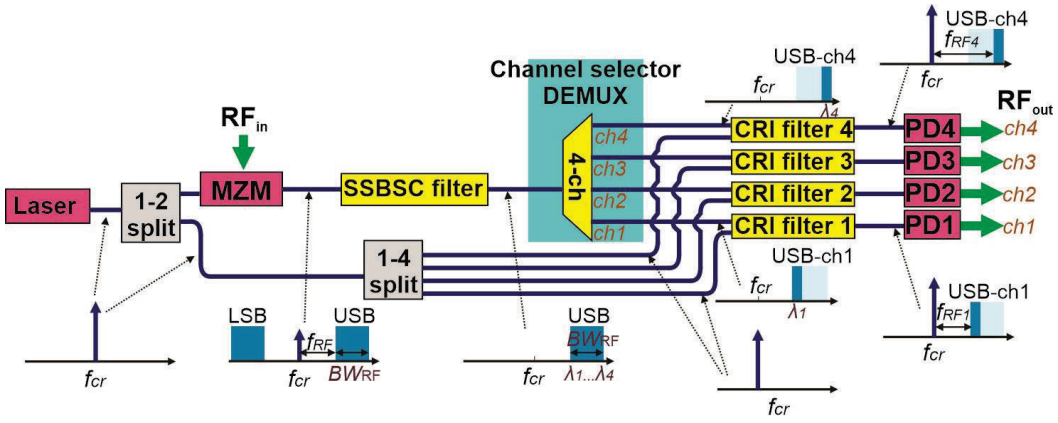

Figure 2. Microwave photonics DEMUX architecture of the proposed channel selector filter.

This is the core architecture for the MWP system. This architecture can be improved by adding one laser for each channel to be demultiplexed to the frequency generation unit. This fact improves the system in terms of reconfigurability and flexibility. Instead of combine the filtered channel after the channel selector DEMUX filter with the split carrier, each channel will be combined with an independent tunable laser. Each laser will act as a local oscillator (LO1, LO2, LO3 & LO4) allowing the tunability of each channel independently and allocate information in any region of the Ka-, Q-, or V-band. As mention before, the main limitation of this approach is the instability due to drifts between each laser. In this paper this drift will be studied as well as alternative techniques to stabilized the lasers and make the system feasible.

3. DEVICE DESCRIPTION

The frequency generation unit will be a laser module. An InP/Si3N4 hybrid integrated dual laser module investigated in this work, which basically is the same structure that will be used for the THORMUX project scope. The device is shown schematically in Figure 3(b). As can be observed, it includes two identical laser structures, which are outlined on the figure using blue dashed boxes labeled Laser1 and Laser2 respectively. Each laser cavity is formed through hybrid integration of an InP Quantum-Well (QW) gain chip (red boxes) and a Si3N4 (proprietary Si3N4 waveguide technology from LioniX International) chip (gray shaded area) using butt-coupling. The InP gain chip is double-pass reflective semiconductor optical amplifier (RSOA) through high-reflective (HR) coating on the leftmost edge, which forms one of the cavity mirrors.

The other mirror is an integrated mirror structure in the Si3N4 substrate, based on a pair of microring resonators (MRR-A and MRR-B) which provide a wavelength tunable optical feedback. The two MRRs have Free Spectral Range (FSR) around 1.6 nm (200 GHz), with slightly different radiuses to enable wavelength tuning through the Vernier effect. In

between the two mirrors, the lasers include a thermally adjustable Phase Tuning Section (PTS) that allows fine tuning of the cavity length for output power maximization and a 2x2 symmetric Mach-Zehnder Interferometer based Thermo-Optic Power Coupler (MZI-TOPC) [14] which allows control of the amount of light fed back to the laser cavity. The Si3N4 waveguides, having a symmetric double-stripe cross section, offer a low propagation loss of about 0.1 dB/cm [15], which allows MRRs to reach Q-factors ranging from 20000 to 200000 [12]. Each laser has an additional I/O control MZI-TOPC which allows to control the amount of the laser optical power that is directed either to the on-chip photodiodes or to an output optical fiber, L1-Out for Laser1 and L2-Out for Laser2. Finally, the on-chip photodiodes include another MZI-TOPC, which allows to control the amount of power from each laser that is directed towards each on-chip photodiode, PD1 and PD2.

A photograph of the InP/Si3N4 hybrid integrated dual laser module is shown in Figure 3(a). As shown in the image, the optical waveguide access ports are coupled to single mode polarization maintaining fibers, which are terminated with an angled facet FC/APC connector to prevent undesired reflections back into the laser cavity.

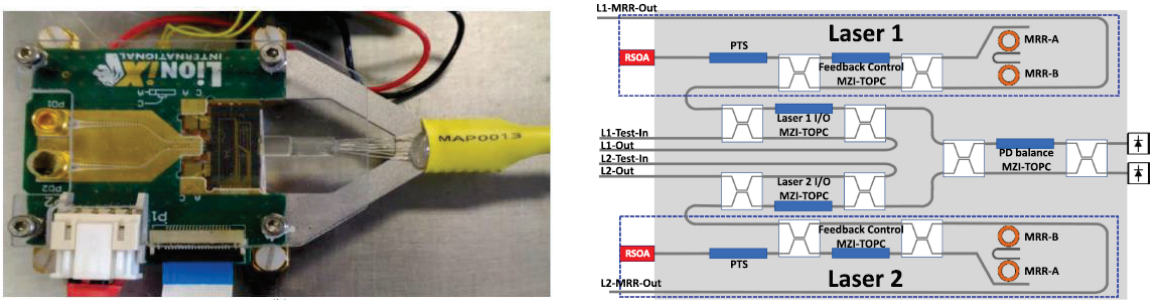

(a) (b)

Figure 3. (a) InP-Si3N4 hybrid integrated dual laser module is assembled on a thermally controlled base. (b) Schematic representation of the device.

4. SETUP DESCRIPTION

The InP-Si3N4 hybrid integrated dual laser module is assembled on a thermally controlled base through a Peltier thermoelectric cooler (TEC) and NTC thermistor. The module is operated between 20°C and 22ºC throughout all the reported measurements. The current injected on the gain section RSOAs is driven from custom battery supply current sources, to reduce the electrical noise, while the heaters in the chip, one per each Mach-Zehnder Interferometer based Thermo-Optic Power Coupler, as well as the heaters from the MRRs are driven from low-noise voltage sources, Keysight E3611.

The device is provided as well with a home-made box entire recovered with isothermal material in order two protect the devices from the environmental conditions and keep the temperature constant Figure 4. The devices are working at Lab temperature (25ºC), where the temperature is supposed to be stable. However, we have seen that the daily temperature fluctuations and the day-night temperature cycles affect to the devices when they are exposed to the environment. With the box we try to reduce these effects.

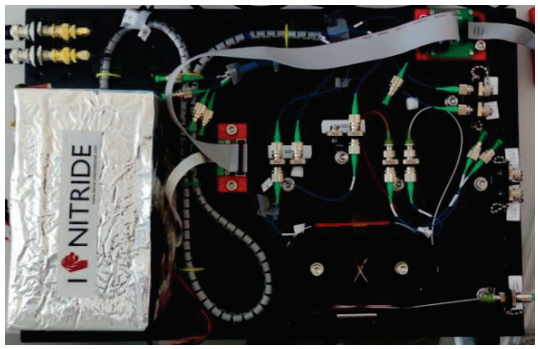

Figure 4. Photograph of the experimental setup for long-term drift measurements including the home-made isothermal box for the InP/Si3N4 hybrid integrated dual laser module

5. EXPERIMENTAL RESULTS

5.1 Frequency Drift.

For the first approach, only the device InP/Si3N4 hybrid integrated dual laser module will be used. The setup will be arranged as shown in Figure 5. The emission wavelength of the lasers is around 1550nm and they can be tuned across the entire optical C-band. Both laser 1 and laser 2 will be injected with a current of 40mA. The H5 and H4 heaters used control the external coupling ratio on both lasers will be biased at 13.632 V and 13.55 V in order to maximize optical power at the output. The heaters that control the wavelength setting H9/H11 and H8/H6 will be biased with a voltage of 0 volts and 11,159 volts, respectively for Laser 1 and Laser 2, so that a difference between the wavelengths is established. 25 GHz emission wave. For this experiment, we are intending to measure the optical drift of each laser and the electrical drift of the generated beat note. As can be seen in the figure, the optical output of each of the lasers will be combined in an optical splitter with a 50/50 ratio. To measure optical and electrical drift simultaneously, an additional 50/50 optical splitter added to the scheme. After the last splitter, the lower optical output ports will be sent to the BOSA high resolution spectrum analyzer to get frequency location of the two optical modes. The upper optical output will be sent to a 50 GHz bandwidth PIN-Photodiode (XPDV2120RA) to perform the opto-electronic conversion and get RF generated frequency.

In the Figure 6 we can observe the temporal evolution of both drifts measured over a period of 12 hours. The figure b shows the optical drift of both lasers. They exhibit an optical drift that ranges from -80 MHz to +520 MHz with respect to the central emission frequency. Figure 6 shows the electrical drift of the generated RF tone. It ranges from -18 MHz to +50 MHz with respect to the initial RF frequency generated by both lasers (25 GHz). It can be notice that the electrical drift is less than the optical. This is due to the fact that, despite the fact that both lasers have independent optical drifts, as they are using the same thermal control, these variations are produced in similar increases and decreases. As the electrical beat note is generated by the frequency difference between Laser 1 and Laser 2 and the displacement due to the drift is synchronize, the electrical drift is reduced.

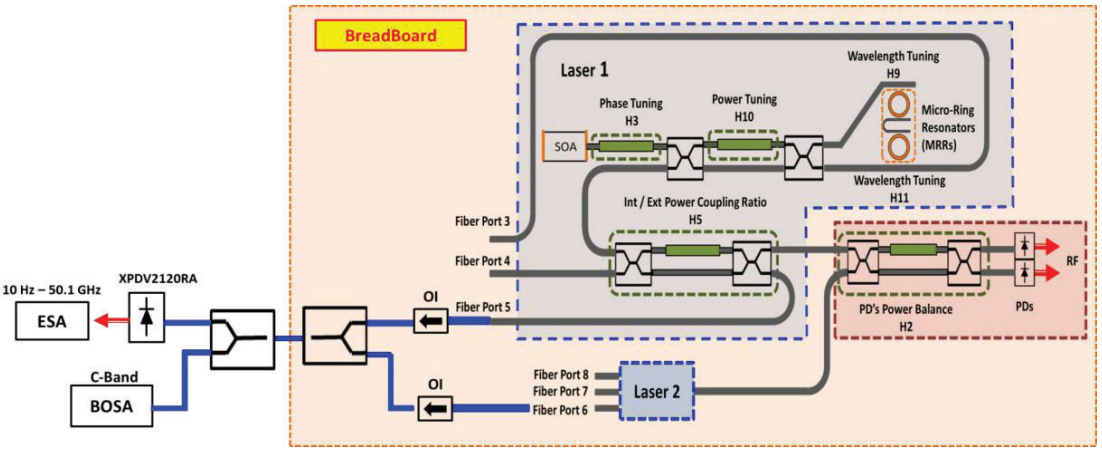

Figure 5. Schematic of the experimental arrangement for frequency drift measurements of the InP/Si3N4 hybrid integrated dual laser module

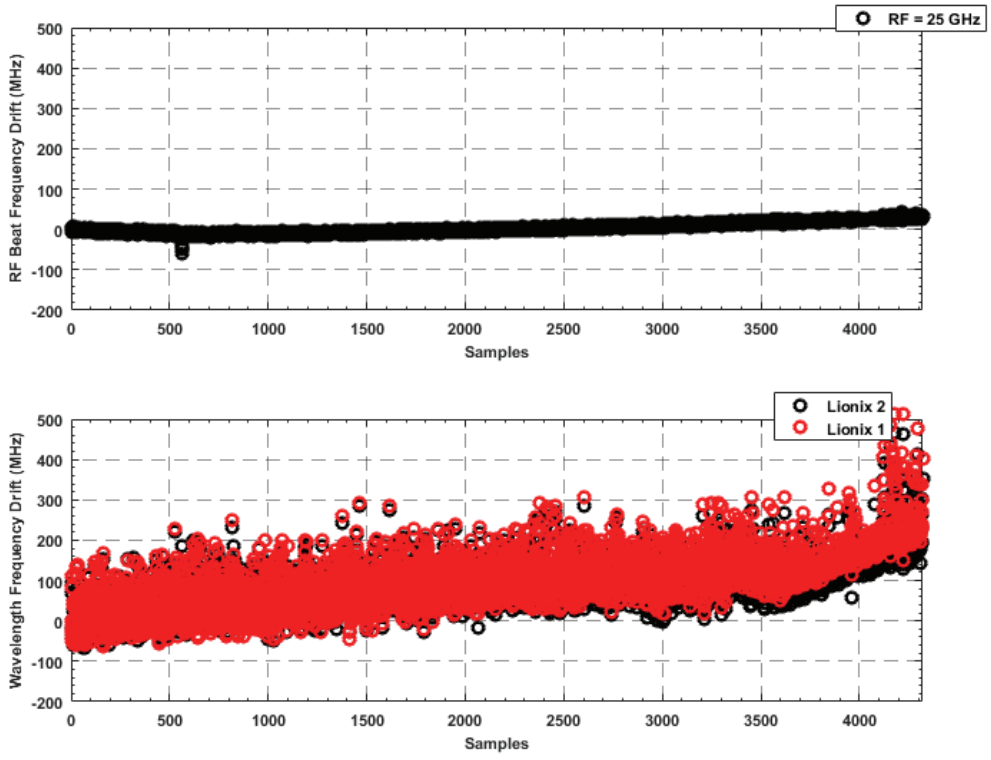

Figure 6. Temporal evolution of the drift of the InP/Si3N4 hybrid integrated dual laser module measured over a period of 12 hours. Optical drift of each laser of the dual module (below). Electrical drift of the generated RF frequency (above)

5.2 Injection Locking Experiments

Measuring the free-running drift is key as it determines the minimum locking range (and, hence, injection ratio) required to maintain the OIL. As the first approach was the one who exhibits the best performance in terms of frequency drift, is the one selected for this experiment. A schematic of the experimental arrangement is showed in the Figure 7(a). Laser 1 will act as slave laser and Laser 2 will be the master. Two OPMs will be used. The one below is used to monitor the injection optical power from the master laser to the slave laser. The one above is connected to an optical port to monitor the slave Laser 1. RSOA section of Laser 1 is supplied with 90 mA, so optical power is 0 dBm. Based on the optical power monitored on the OPM2, the optical power injected from the master laser to the slave laser is -3 dBm. Therefore, for this experiment we have an Injection Ratio of -3 dB. Heater H5 is biased at 13.632V. By this way the MZM is connected in through and amount of light passing from laser 2 to laser 1 is maximized. A detailed description of the emission wavelength selection for this type of lasers can be found in [18]. However, this wavelength selection was characterized in 1 nm step (which in terms of frequency means 125 GHz). This is 5 orders of magnitude above what is required to perform this experiment. A new look-up table around the working area was done based on the previous characterization showed in [19]. Heaters H9/H11 were biased at zero volts to keep the wavelength of the slave laser fixed, Figure 7(b). The H8/H6 heaters was sweep between 11.09V to 12.09 volts. Over this range of voltages, a region within the optical spectrum where the master laser can be continuously tuned above the slave laser was founded, Figure 7(c). As Laser 2 gets closer to Laser 1 we see that side-modes rises. This happens when he hybrid laser was outside the locking range. Numerous intermodulation products appeared at the BOSA. When locked was achieved a clean and stable signal was visible at the BOSA. Over these conditions a locking-range of 1.86 GHz was achieved which is sufficient enough to ensure that the laser will be stabilized at the worst case of drift.

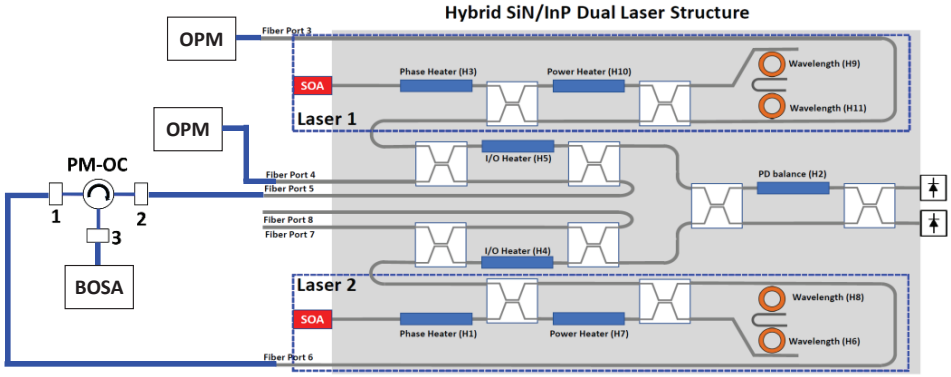

(a)

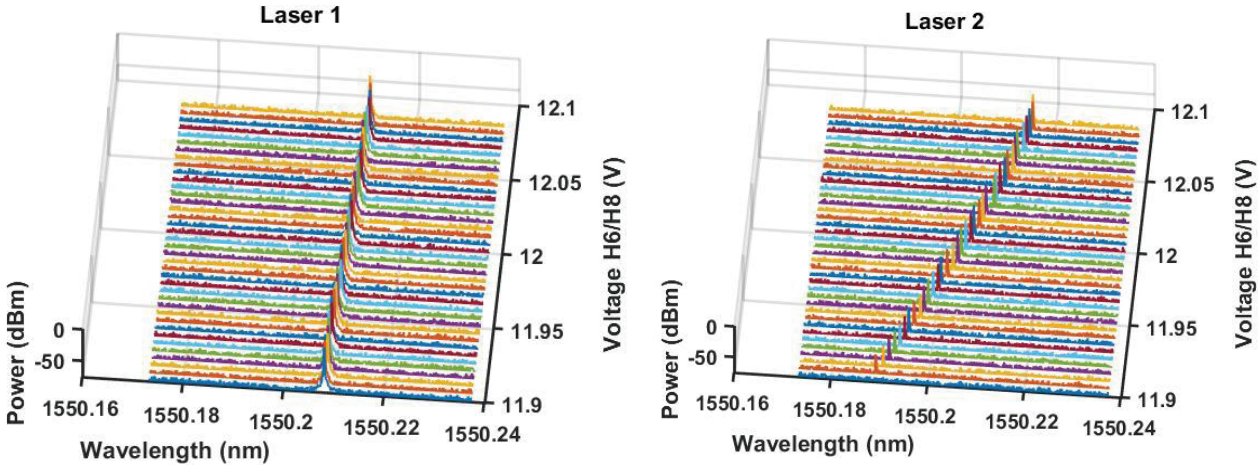

(b) (c)

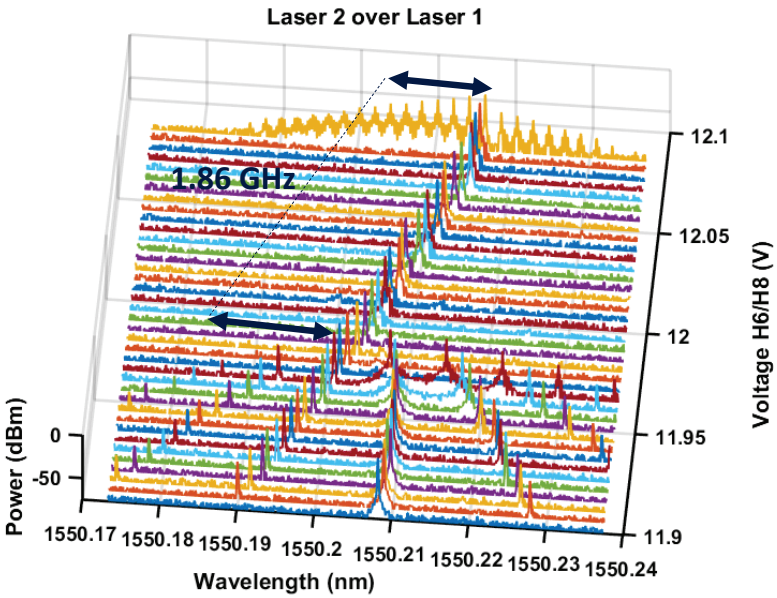

(d)

Figure 7. Experimental arrangement for optical injection-locking (OIL) experiment of Laser2 over Laser1. (b) Optical spectrum evolution of Laser 1 when sweeping H6/H8. (c) Optical spectrum of Laser 2 when sweeping H6/H8. (d) Optical spectrum of the OIL experiment when Laser 2 injects over Laser 1

6. CONCLUSIONS

In this paper, on the one hand, we have presented a frequency stability study of integrated hybrid lasers. Despite the drifts in the optical domain are around 400-520 MHz. As lasers are integrated in the same chip, they are under the same thermal controller. The TEC acts over both lasers at same time making thermal fluctuations very similar on each laser. This factor results on RF frequencies with drifts not greater than 50 MHz. On the other hand, we have present and experiment for the first time of optical injection of an InP-Si3N4 integrated laser on-chip from another integrated in the same chip for the first time. Over certain current supply and bias condition we have demonstrated that with an Injection Ratio -3 dB, a locking range of 1.86 GHz has been achieved. This value is almost three times above the 500 MHz worst case drift values presented during this study. This fact eliminated the necessity of using an external laser to generated the optical frequency comb reducing the SWaP. We have demonstrated that for a fully reconfigurable approach one of the integrated laser can be used to lock the rest in order to stabilize the entire system.

ACKNOWLEDGMENT

This work has been supported by the European Space Agency (ESA) within the TRP program “Tuneable Photonic RF Demultiplexer for Broadband Satellites - THORMUX” and by H2020 within the program “SpaceBeam”, Contract no. 870421 and by an RFP named “Integrated microwave photonic technology for wide-frequency tuning signal generation” within the “OSIP” (The Open Space Innovation Platform) program. This work was also supported by the CONEX-Plus project, which is funded by UC3M and the European Commission through the Marie-Sklodowska Curie COFUND Action (H2020-MSCA-COFUND-2017- GA 801538).

REFERENCES

[1] S. Vono, G. Di Paolo, M. Piccinni, A. Pisano, M. Sotom, M. Aveline, P. Ginestet, "Towards telecommunication payloads with photonic technologies," Proc. SPIE 10563, International Conference on Space Optics ICSO 2014
[2] S. Roux et al., "Advanced photonic payloads for broadband telecom satellites: Integration and tests of a representative repeater demonstrator," Proc. SPIE 11180, International Conference on Space Optics ICSO 2018
[3] Georgios Charalambous and Stavros Iezekiel, "Microwave photonic frequency generation and conversion unit design for Ka-band satellite payloads," Proc. SPIE 11852, International Conference on Space Optics ICSO 2020
[4] Ronald T. Logan Jr., Davinder Basuita, "Photonic components for spacecraft fiber optic datalinks and free-space optical communications terminals," Proc. SPIE 11852, International Conference on Space Optics ICSO 2020
[5] Javad Anzalchi et al., "Towards demonstration of photonic payload for telecom satellites," Proc. SPIE 11180, International Conference on Space Optics ICSO 2018
[6] D. Marpaung, J. P. Yao, et al., "Integrated microwave photonics," Nature Photonics 13, 80 (2019).
[7] T. Nagatsuma, H. Ito and K. Iwatsuki "Generation of Low-phase Noise and Frequency-tunable Millimeter-/terahertz-waves Using Optical Heterodyning Techniques with UTC-PD," Proc. of 36th European Microwave Conference, 2006.
[8] M. Lo, A. Zarzuelo, R. Guzmán and G. Carpintero, "Monolithically Integrated Microwave Frequency Synthesizer on InP Generic Foundry Platform," in Journal of Lightwave Technology, vol. 36, no. 19, pp. 4626-4632, Oct.1, 2018
[9] T. Nagatsuma and G Carpintero "Recent Progress and Future Prospect of Photonics-Enabled Terahertz Communications Research" IEICE Trans. On Electronics E98-C (12), 1060 (2015).
[10] L. Gonzalez-Guerrero et al., "InP-Si3N4 Hybrid Integrated Optical Source for High-purity Mm-wave Communications," 2022 Optical Fiber Communications Conference and Exhibition (OFC), 2022, pp. 1-3.
[11] K. Balakier et al., "Optical injection locking of monolithically integrated photonic source for generation of high purity signals above 100 GHz" Optics Express 22, 29404 (2014).
[12] G. Carpintero, S. Hisatake, D. De Felipe, R. Guzman, T. Nagatsuma, and N. Keil, "Wireless Data Transmission at Terahertz Carrier Waves Generated from a Hybrid InP-Polymer Dual Tunable DBR Laser Photonic Integrated Circuit," Scientific Reports 8, (2018).
[13] J. J. O'Reilly, P. M. Lane, R. Heidemann and R. Hofstetter, "Optical generation of very narrow linewidth millimeter wave signals," Electron. Lett. 28, 2309 (1992).
[14] T. Nagatsuma et al, "Photonic generation of Millimeter and Terahertz waves and its applications," Automatika 49, 51 (2008).
[15] A. Stöhr et al, "Millimeter-Wave Photonic Components for Broadband Wireless Systems," IEEE Trans. Microwave Theory and Techniques 58, 3071 (2010).
[16] J. J. O'Reilly and P. M. Lane, "Remote delivery of video services using mm-wave and optics," J. Lightwave Technol. 12, 369 (1994).
[17] J. J. O'Reilly and P. M. Lane, "Fiber-supported optical generation and delivery of 60 GHz signals," Electron. Lett. 30, 1329 (1994).
[18] Y. Fan et al., "290 Hz intrinsic linewidth from an integrated optical chip-based widely tunable InP-Si3N4 hybrid laser," in Proc. Conf. Lasers Electro-Opt., 2017, Paper. JTh5C.9.
[19] R. Guzmán *et al*., "Widely Tunable RF Signal Generation Using an InP/Si3N4 Hybrid Integrated Dual-Wavelength Optical Heterodyne Source," in *Journal of Lightwave Technology*, vol. 39, no. 24, pp. 7664-7671, 15 Dec.15, 2021